Journal of Organometallic Chemistry 736 (2013) 19–26

Contents lists available at SciVerse ScienceDirect

Journal of Organometallic Chemistry

journal homepage: www.elsevier.com/locate/jorganchem

Synthesis, characterization and antiplasmodial evaluation of cyclopalladated thiosemicarbazone complexes

Muneebah Adams [a], Carmen de Kock [b], Peter J. Smith [b], Kelly Chibale [a,c], Gregory S. Smith [a,*]

[a] Department of Chemistry, University of Cape Town, Private Bag, Rondebosch 7701, South Africa
[b] Division of Pharmacology, Department of Medicine, University of Cape Town, K45, OMB, Groote Schuur Hospital, Observatory 7925, South Africa
[c] Institute of Infectious Disease and Molecular Medicine, University of Cape Town, Rondebosch 7701, South Africa

ARTICLE INFO

Article history:
Received 28 December 2012
Received in revised form
13 February 2013
Accepted 19 February 2013

Keywords:
Bioorganometallic chemistry
Thiosemicarbazone
Cyclopalladation
Antiplasmodial activity

ABSTRACT

Cyclopalladated thiosemicarbazone complexes arising through chelation of the tridentate thiosemicarbazone ligand via the *ortho*-carbon of the aryl ring, the imine nitrogen and the thiolate sulfur were synthesized with the phosphorus ligand occupying the fourth coordination site of the palladium(II) ion. These complexes were prepared by cleavage of the bridging Pd–S bonds of previously reported tetranuclear complexes with phosphorus ligands such as PTA and aminophosphines. The cyclopalladated complexes along with their free ligands were screened for antiplasmodial activity against two *Plasmodium falciparum* strains, NF54 (chloroquine-sensitive) and Dd2 (chloroquine-resistant), exhibiting inhibitory effects in the low micromolar range.

1. Introduction

Probing the application of platinum group metal-based compounds as biological agents has increased exponentially within the field of inorganic and organometallic research [1–4]. One of the leading diseases being targeted by researchers is malaria, an infectious parasitic disease estimated to have affected over 200 million people in 2010 [5]. However, despite the success of antimalarial drug regiments, these treatments are steadily losing their efficacy as resistance to current drug treatments increases [6]. This has led to the search for new and effective antimalarial drugs, particularly to combat the rising resistance [7–9].

Thiosemicarbazones are Schiff-base compounds well-known for their pharmacological properties, such as antitumour [10–15], antiviral [16,17], antibacterial [18] and especially for their use as antiparasitic [10,11,19–24] agents. Their ability to chelate endogenous metals such as Fe(III) which may be required for the function of certain metal dependent enzymes, inhibits parasite growth [25,26].

On the other hand, chemistry associated with the preparation of cyclometallated complexes is well established, especially those prepared via C–H activation [27–32]. The cyclopalladated system reported herein is brought about through oxidative addition of the *ortho* C–H bond of an aryl group present in the ligand (Fig. 1). However, in addition to the aforementioned method, cyclometallation may occur through transmetallation (via lithiation of the starting compound) as well the oxidative addition of a C–Br bond [27,32]. The biological evaluation of these types of complexes is still relatively new, though promising results have been reported [10,33,34].

This study aims to expand on work previously carried out within our research group on cyclopalladated complexes [19]. The new cyclopalladated thiosemicarbazone complexes reported herein are discussed in terms of the synthesis, characterization and antiplasmodial evaluation.

2. Results and discussion

2.1. Synthesis and characterization of phosphine ligands and the palladium(II) complexes

The iminophosphine ligand (**L1**) is a known compound synthesized via a reported method [35]. The iminophosphine ligand **L2** was prepared via a Schiff-base condensation reaction between (2-diphenylphosphino)benzaldehyde and *p*-phenylenediamine in methanol (Scheme 1) [33–35]. Reduction of the iminophosphine ligands (**L1**, **L2**) using sodium borohydride produced the aminophosphine ligands (**L3**, **L4**). The phosphine ligands (**L1**, **L3**) were

* Corresponding author.
E-mail address: Gregory.Smith@uct.ac.za (G.S. Smith).

0022-328X/$ – see front matter © 2013 Elsevier B.V. All rights reserved.
http://dx.doi.org/10.1016/j.jorganchem.2013.02.024

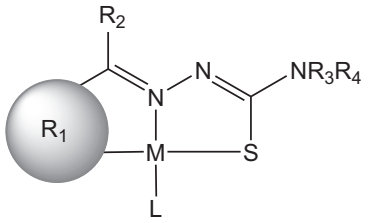

Fig. 1. The general structure of a cyclometallated complex. M = metal; L = ligand; R_1 = aryl group; R_2, R_3, R_4 = H, alkyl or aryl group.

isolated as yellow oils, whereas the diphosphine ligands (**L2**, **L4**) were isolated as yellow solids, in relatively high yields (88–94%). These aminophosphine ligands along with 1,3,5-triaza-7-phosphaadamantane (PTA) were the phosphorus-donor ligands chosen as precursors for the targeted cyclopalladated complexes.

The known thiosemicarbazone ligands, 3,4-dichloroacetophenone thiosemicarbazone (**L5**) and 3,4-dichloropropiophenone thiosemicarbazone (**L6**), were used in the synthesis of the reported tetranuclear complexes [Pd(3,4-dichloroacetophenone thiosemicarbazone)]$_4$ (**1**) and [Pd(3,4-dichloropropiophenone thiosemicarbazone)]$_4$ (**2**) [19,36]. The molecular structures of **1** and **2** have not been reported before.

The synthesis of complexes **3**–**6** was accomplished through cleavage of the bridging Pd–S bond (Scheme 2) in the core of the tetranuclear complex (**1**, **2**) by the appropriate phosphorus-containing ligand. Complexes **3**–**6** were isolated as yellow solids in moderate to high yields in the range 40–94%.

In the ^{1}H NMR spectra of the iminophosphine ligands **L1** and **L2**, the signal corresponding to the imine proton is observed as a doublet ($^4J_{HP} \sim 5.00$ Hz) at *ca.* 9.00 ppm. Reduction of the imine bond using sodium borohydride is confirmed by the absence of the imine peak in the ^{1}H NMR spectra of **L3** and **L4**, and the appearance of the signals for the $-C\underline{H}_2-N$ and secondary amine ($CH_2-N\underline{H}-$) protons. The signals for the aromatic protons are observed in the range 6.76–8.19 ppm. The protons of the propyl chain are observed upfield in the aliphatic region. For compound **L3**, the CH_3 protons are observed as a triplet ($J = 7.44$ Hz) at 0.73 ppm due to coupling with the adjacent CH_2 protons. The $-CH_2-$ protons are observed as a multiplet at 1.26 ppm for **L3**, while the remaining $N-CH_2-$ protons are observed as a triplet ($J = 7.40$ Hz) at 2.39 ppm. The protons of the rigid aromatic spacer are observed as a singlet at 6.88 and 6.14 ppm for compounds **L2** and **L4** respectively. The observation of a singlet is due to the symmetry of the compounds about a two-fold rotation axis.

Compounds **L3** and **L4** are similar in structure and thus comparable trends were observed in the $^{13}C\{^1H\}$ NMR spectra. In the $^{13}C\{^1H\}$ NMR spectra of **L3** and **L4**, several carbon atoms situated close to phosphorus are observed as doublets due to coupling with phosphorus. For compounds **L3** and **L4**, the signal for $\underline{C}H_2-NH$ is observed as a doublet at 52.7 ($^3J_{CP} = 20.7$ Hz) and 46.1 ppm ($^3J_{CP} = 25.7$ Hz) respectively due to the three bond coupling experienced with phosphorus. The signals for the carbon atoms of the propyl chain are observed in the aliphatic region at 51.4, 23.2 and 11.9 ppm respectively for compound **L3**. The aromatic carbons of the rigid spacer in compound **L4** are observed as singlets at 139.7 and 113.5 ppm, which corroborate the statement that the compound is symmetrical.

Further confirmation is given by the singlets displayed in the $^{31}P\{^1H\}$ NMR spectra, where the signals shifted upfield from −13.9 (**L1**) and −12.2 (**L2**) ppm to −16.1(**L3**) and −16.9 (**L4**) ppm respectively. Infrared spectral analysis of the iminophosphine ligand **3** revealed an absorption band at 1610 cm^{-1} for the imine (C=N) bond. No absorption band is observed in the region characteristic of C=N stretchings for the aminophosphine ligands **L3** and **L4**, whilst a weak absorption band is observed at 3405 and 3427 cm^{-1} respectively, in the region for N–H stretching frequency of secondary amines. This confirms reduction of the C=N bond. EI$^+$-mass spectra displayed molecular ion peaks at *m*/*z* 653 and 656 respectively for **L2** and **L4**.

Cleavage of the bridging Pd–S bond by the phosphine ligands is seen in the ^{1}H NMR spectra (**3**, **5**, **6**) where the signal for the aromatic proton H_a is now observed as a doublet ($^4J_{HP} \sim 3.66$ Hz) between 6.13 and 7.10 ppm, while the signal for **4** is observed as a broad signal. Compounds **3** and **4** contain the PTA ligand, and thus a singlet associated with the $PC\underline{H}_2N$ protons was observed at *ca.* 4.27 ppm. The $NC\underline{H}_2N$ protons are in an AB spin system resulting in two doublets corresponding to the different environments experienced by the axial and equatorial $NC\underline{H}_2N$ protons [37–39]. The doublet associated with the protons in the axial and equatorial protons are observed around 4.44 and 4.58 ppm respectively for **3** and **4**. In the ^{1}H NMR spectra of **4** and **5**, the aromatic protons are observed in the range 7.00–7.74 ppm. Compound **5** maintains the two-fold symmetry displayed by **L2** and **L4** which is evident by the singlet observed for the protons of the aromatic spacer.

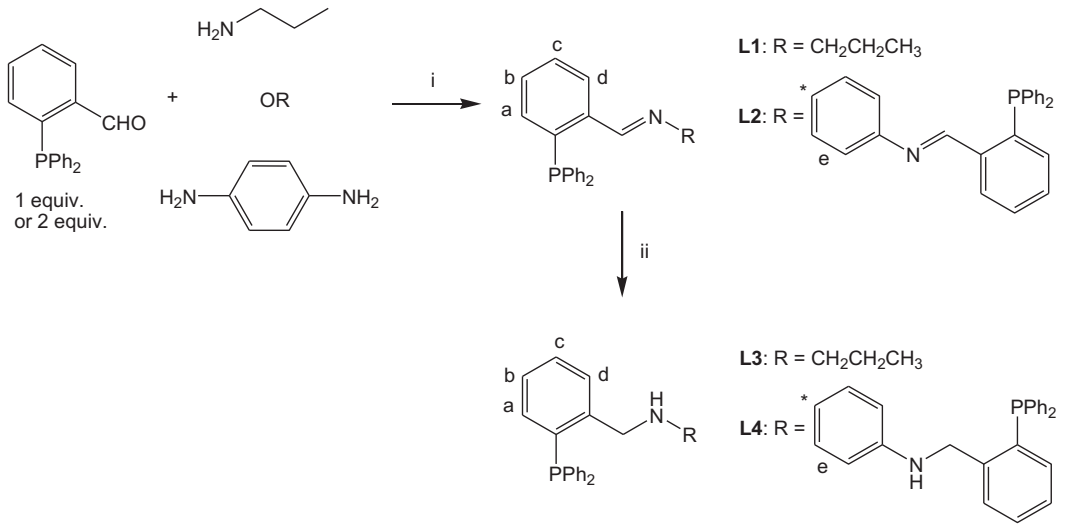

Scheme 1. (i) **L2**: MeOH, reflux, 6 h; (ii) **L3**: MeOH, $NaBH_4$, ambient temp. 3 h; **L4**: DCM:MeOH (75:25% v/v), $NaBH_4$, ambient temp. 6 h.

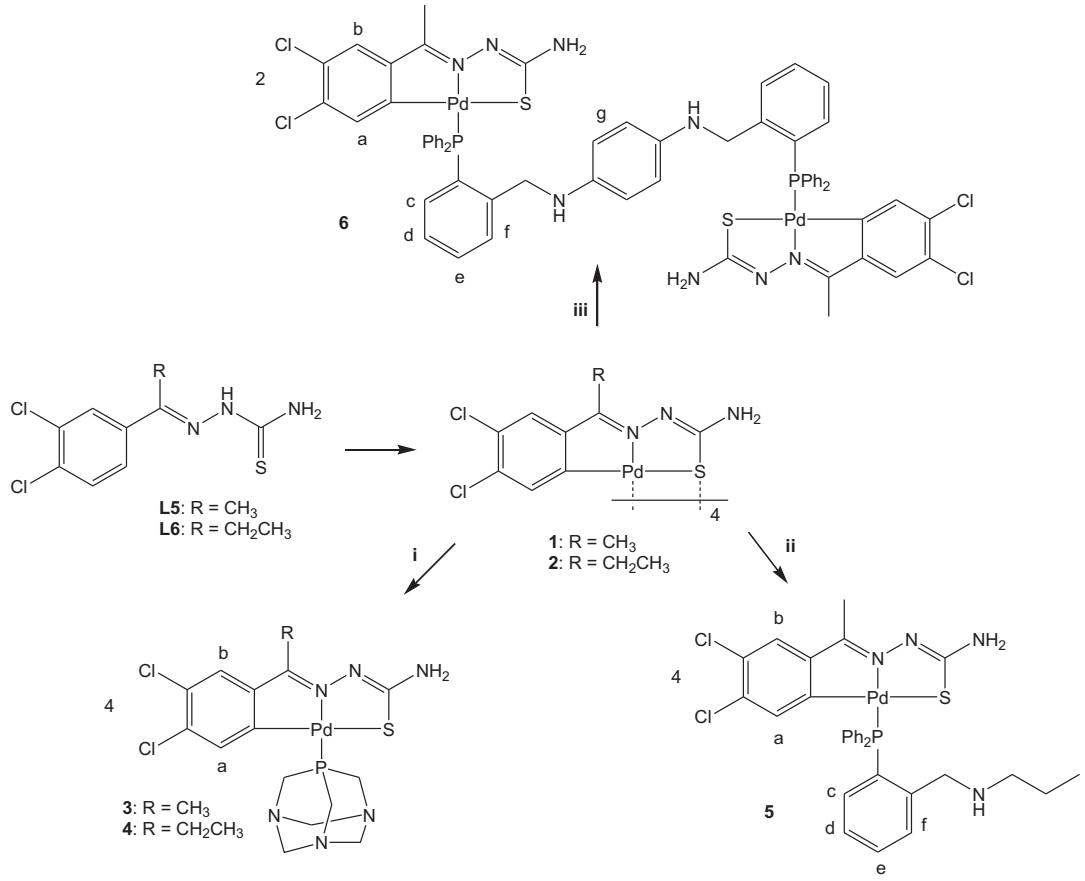

Scheme 2. (i) Acetone, PTA (4 equiv.), reflux, 3 h; (ii) Acetone, **L3** (4 equiv.), ambient temp. 3 h; (iii) Acetone/DCM, **L4** (2 equiv.), ambient temp. 5 h.

The $^{13}C\{^{1}H\}$ NMR spectra displayed the signal for the thiolate carbon downfield at *ca.* 177.0 ppm when compared to that observed for the tetranuclear complexes. A doublet ($^{4}J_{HP} \sim 9.76$ Hz) is displayed in the spectra for **5** and **6**. The imine carbons are observed in the range 163.6–172.4 ppm while the aromatic carbon atoms resonate in the range 114.0–164.0 ppm. As seen with other complexes containing the PTA ligand, the carbon atoms N$\underline{C}$H$_2$N and P$\underline{C}$H$_2$N resonate as doublets at 72.4 ($^{3}J_{CP} = 7.40$ Hz) and 51.5

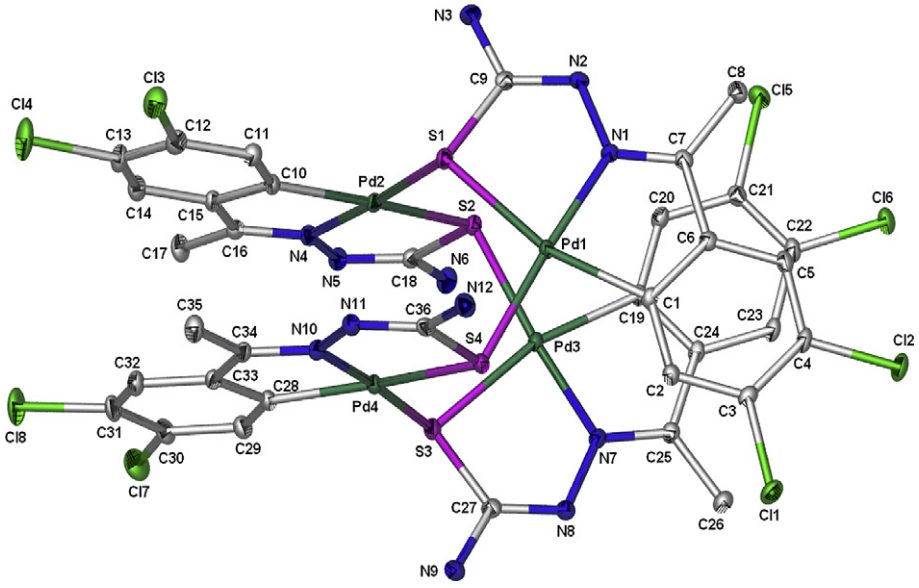

Fig. 2. The molecular structure of **1**. Hydrogen atoms have been omitted for clarity. Selected bond lengths (Å) and angles (°): Pd(1)–N(1) 2.002(3); Pd(1)–C(1) 1.998(3); Pd(1)–S(1) 2.3637(9); Pd(1)–S(4) 2.3194(9); S(1)–C(9) 1.787(4); N(1)–C(7) 1.303(4); N(2)–C(9) 1.303(4); N(1)–Pd(1)–C(1) 81.24(13); N(1)–Pd(1)–S(1) 83.15(8); S(4)–Pd(1)–S(1) 100.56(3); C(1)–Pd(1)–S(4) 94.91(10); N(1)–Pd(1)–S(4) 175.63(8); C(1)–Pd(1)–S(1) 164.06(11).

Table 1
Crystal data and structure refinement data for complexes **1**, **4** and **5**.

	$1.3C_4H_8O$	**4**	$5.2CHCl_3$
Empirical formula	$C_{48}H_{52}Cl_8N_{12}O_3Pd_4S_4$	$C_{16}H_{21}Cl_2N_6PPdS$	$C_{33}H_{33}Cl_8N_4PPdS$
Formula weight	1682.46	537.72	938.66
Temperature (K)	173(2)	173(2)	173(2)
Wavelength (Å)	0.71073	0.71073	0.71073
Crystal system	Monoclinic	Monoclinic	Triclinic
Space group	*P*21/*n*	*C*2/*c*	*P*-1
a (Å)	16.4634(9)	35.7802(19)	11.7431(9)
b (Å)	9.1883(5)	6.9559(4)	12.8847(11)
c (Å)	38.962(2)	16.2229(9)	14.7987(11)
α (°)	90	90	69.656(2)
β (°)	93.4590(10)	92.3610(10)	84.069(2)
γ (°)	90	90	72.202(2)
V (Å^3)	5883.1(6)	4034.2(4)	1999.0(3)
Z	4	8	2
D_{calc} (Mg m^{-3})	1.900	1.771	1.542
Absorption coefficient (mm^{-1})	1.762	1.383	1.120
F (000)	3328	2160	924
Crystal size (mm^3)	0.18 × 0.17 × 0.16	0.09 × 0.08 × 0.07	0.07 × 0.08 × 0.12
θ Range for data collection (°)	2.06–28.40	2.28–28.44	1.8–28.3
Index range	$-22 \le h \le 19$; $-10 \le k \le 12$; $-52 \le l \le 52$	$-47 \le h \le 47$; $-9 \le k \le 9$; $-21 \le l \le 21$	$-15 \le h \le 14$; $-17 \le k \le 17$; $-11 \le l \le 19$
Reflections collected	67,481	35,350	21,501
Independent reflections [*R*(int)]	14,734 [0.0604]	5077 [0.0666]	9946 [0.041]
Data/restraints/parameters	14,734/0/723	5077/0/244	9946/21/414
Goodness-of-fit on F^2	1.011	1.009	1.042
Transmission	0.7658, 0.7422	0.9094, 0.8857	0.9256, 0.8772
Final *R* indices [$I > 2\sigma(I)$]	$R_1 = 0.0365$, $wR_2 = 0.0681$	$R_1 = 0.0291$, $wR_2 = 0.0586$	$R_1 = 0.0664$, $wR_2 = 0.1719$
R indices (all data)	$R_1 = 0.0598$, $wR_2 = 0.0758$	$R_1 = 0.0443$, $wR_2 = 0.0644$	$R_1 = 0.0928$, $wR_2 = 0.1909$
Largest difference in peak and hole (e Å^{-3})	0.722 and −0.520	0.469 and −0.457	1.98 and 1.51

($^1J_{CP}$ = 15.5 Hz) ppm for **3** and **4**. The −C̲H$_2$−N carbon atom of compound **5** and **6** resonates as a doublet at 52.8 ($^3J_{CP}$ = 12.8 Hz) and 47.9 ($^3J_{CP}$ = 14.8 Hz) ppm respectively [37–39].

For the phosphorus-containing cyclopalladated complexes (**3**–**6**), a singlet was observed in the $^{31}P\{^1H\}$ NMR spectra at −49.5, −49.6, 29.5 and 29.0 ppm respectively, which is downfield from the free phosphine ligands. Infrared spectral analysis of **3**–**6** displayed two absorption bands in the region typical of C=N bonds between 1559 and 1641 cm^{-1}. The lower energy absorption band corresponds to the metal-coordinated imine (through the nitrogen atom), while the higher energy absorption band is assigned to the newly formed C=N bond.

EI$^+$- and ESI$^+$-mass spectra were recorded for compounds **3**–**6**, which displayed a peak corresponding to the molecular ion.

2.2. Molecular structures of *1*, *4* and *5*

Single crystals, crystallized with three molecules of tetrahydrofuran, were obtained via the slow evaporation of a solution of compound **1** dissolved in tetrahydrofuran/hexane. Single crystals of 4 were obtained by the slow diffusion of hexane into a tetrahydrofuran solution of 4. The slow diffusion of hexane into a solution of **5** dissolved in chloroform allowed for the formation of suitable crystals with two molecules of chloroform. The molecular structures of **1**, **4** and **5** were elucidated using single-crystal X-ray diffraction and validates the spectroscopic and analytical characterization of the mononuclear (**4** and **5**) complexes, as well as the molecular structure of the previously described tetranuclear complex **1** which has not yet been reported. The molecular structure of **1**, **4** and **5** are shown in Figs. 2–4 and the crystallographic data is given in Table 1.

Compound **1** and **4** crystallizes in a monoclinic system with space groups *P*21/*n* and *C*2/*c* respectively, while compound **5** is packed in a centrosymmetric triclinic system with *P*-1 space group. The formation of the expected two 5-membered rings are observed as the thiosemicarbazone ligand chelates to the palladium(II) centre in a tridentate *C*,*N*,*S*-mode [10,49]. Upon formation of compound **1**, the bonds N(1)–C(7) and N(2)–C(9) have equal bond lengths of 1.303(4) Å, which confirms the formation of the second C=N bond (Fig. 2). Upon formation of the mononuclear complexes, the fourth coordination site on the metal is occupied by the phosphorus ligand. The metal-coordinated imine bond is slightly shorter than that observed for compound **1**, while the second C=N bond is slightly longer (Figs. 2–4). The chelation of the ligand in the thiolate form is confirmed when comparing the length of the S–C bond to that of other thiosemicarbazone ligands and palladium(II) complexes. Complexes **1**, **4** and **5** have S–C bond lengths of 1.787(4), 1.768(3) and 1.755(6) respectively. Previously published molecular structures reported bond lengths of approximately 1.684 Å for the ligand and 1.782 Å for the palladium(II) complexes [40,41]. The S–C bond lengths reported for complexes **1**, **4** and **5** is consistent with single bond character, i.e. chelation in the thiolate form. The lengthening of the Pd–N bonds of compounds **4** (2.022(2) Å) and **5** (2.033(5) Å) compared to compound **1** (2.002(3) Å) is indicative of the *trans* effect induced by the introduction of a phosphorus ligand.

Compounds **1**, **4** and **5** have a slightly distorted square-planar geometry around the palladium(II) centre (Figs. 2–4). The bond angles between adjacent coordinating atoms are close to the expected value of 90°, in the range 80.71(10)–101.45(8)°. This observed geometry is comparable to that in related complexes [19,29,42,43].

2.3. Antiplasmodial activity

The thiosemicarbazone ligands (**L5**, **L6**) and their corresponding cyclopalladated complexes (**1**–**6**) were evaluated for antiplasmodial

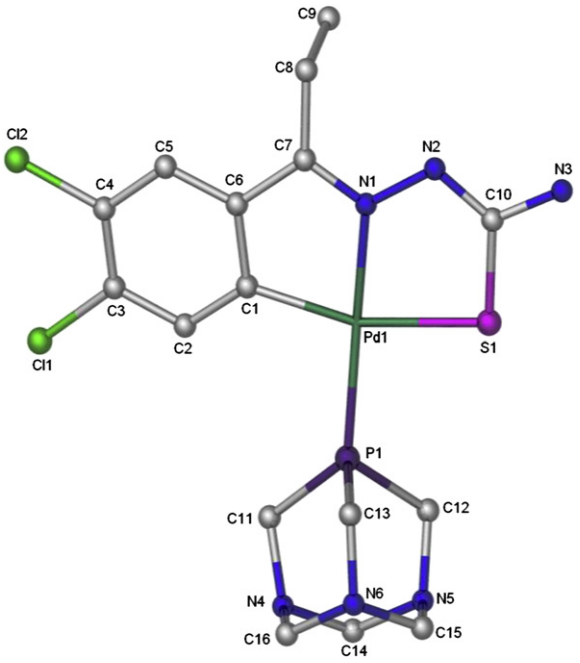

Fig. 3. The molecular structure of **4**. Hydrogen atoms have been omitted for clarity. Selected bond lengths (Å) and angles (°): Pd(1)–N(1) 2.022(2); Pd(1)–C(1) 2.024(3); Pd(1)–P(1), 2.2412(7); Pd(1)–S(1) 2.3397(7); S(1)–C(10) 1.768(3); N(2)–C(10) 1.310(3); N(1)–C(7) 1.302(3); N(1)–Pd(1)–C(1) 80.71(10); N(1)–Pd(1)–S(1) 83.19(6); C(1)–Pd(1)–P(1) 101.45(8); P(1)–Pd(1)–S(1) 95.16(2); C(1)–Pd(1)–S(1) 163.28(8); N(1)–Pd(1)–P(1) 170.63(6).

activity against the *Plasmodium falciparum* strains, NF54 (chloroquine-sensitive) and Dd2 (chloroquine-resistant). The control drug used in the experiment was chloroquine diphosphate (CQDP), and the results are displayed in Table 2. Compounds **L5** and **L6** were more active in the Dd2 strain (4.46 and 9.82 μM respectively) than in the NF54 strain (14.1 and 19.0 μM respectively), The tetranuclear complexes **1** and **3** (Scheme 2) were inactive against the NF54 and Dd2 strains at the highest tested concentrations (1000 ng/ml).

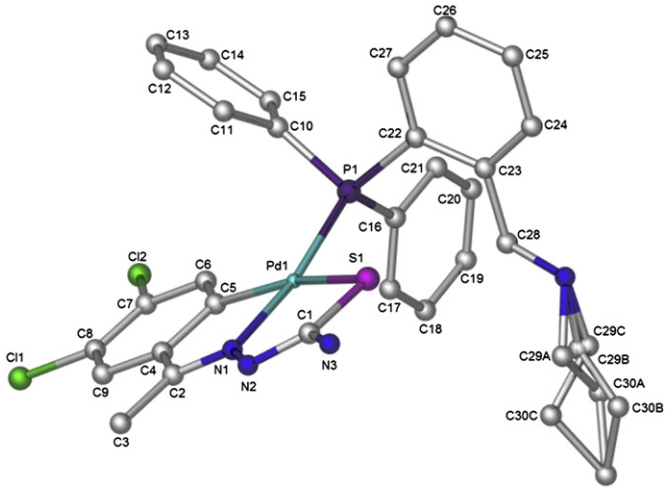

Fig. 4. The molecular structure of **5**. Hydrogen atoms have been omitted for clarity. The propyl chain was disordered and the carbon atoms 29 and 30 were refined with equal site occupancy factors of one-third each. Selected bond lengths (Å) and angles (°): Pd(1)–N(1) 2.033(5); Pd(1)–C(5) 2.029(4); Pd(1)–P(1) 2.2571(14); Pd(1)–S(1) 2.3181(15); S(1)–C(1) 1.755(6); N(2)–C(1) 1.331(8); N(1)–C(2) 1.298(7); N(1)–Pd(1)–C(5) 81.34(18); N(1)–Pd(1)–S(1) 83.24(13); C(5)–Pd(1)–P(1) 96.42(14); P(1)–Pd(1)–S(1) 99.11(5); C(5)–Pd(1)–S(1) 164.47(14); N(1)–Pd(1)–P(1) 171.14(15).

Table 2
IC_{50} values for compounds **L5**, **L6** and **1**–**6** against the *P. falciparum* strains NF54 (CQS) and Dd2 (CQR).

IC_{50} [a] (μM)			
Compound	NF54	Dd2	RI[b]
L5	14.1 ± 0.34	9.82 ± 0.78	0.70
L6	19.0 ± 2.18	4.46 ± 0.74	0.23
1	Inactive	Inactive	ND[c]
2	Inactive	Inactive	ND
3	1.93 ± 0.04	2.69 ± 0.22	1.39
4	1.81 ± 0.11	1.73 ± 0.16	0.96
5	1.76 ± 0.074	1.59 ± 0.053	0.90
6	Inactive	54.56 ± 3.83	ND
CQDP	0.031 ± 0.006	0.22 ± 0.016	7.10

[a] IC_{50}: compound concentration causing 50% inhibition of parasitaemia *in vitro*.
[b] RI: resistance index = [IC_{50} (Dd2)]/[IC_{50} (NF54)].
[c] ND: not determined.

On the other hand compounds **3**–**5** exhibit comparable inhibitory activity in both strains, with IC_{50} values in the range 1.59–2.69 μM. An enhancement of activity is clearly observed for the mononuclear complexes (**3**–**5**) compared to the free monothiosemicarbazone ligands (**L5**, **L6**).

The rationale behind the synthesis of polynuclear complexes was to determine if an enhancement in antiplasmodial activity would be observed with an increase in the number of metal centres. However, the data collected for polynuclear complexes should be read with caution before a definite correlation can be made between the activity displayed and the number of metal centres. Compound **6**, which contains a diphosphine ligand, allowing for the synthesis of a binuclear complex, exhibits only moderate activity (IC_{50} = 54.56 ± 3.83 μM) against the Dd2 strain in comparison to the mononuclear complexes **3**–**5**. However, against the NF54 strain compound **6** displays weak potency at the tested concentration (1000 ng/ml). Based on the data available for the Dd2 strain, the proposed enhancement of activity is not observed moving from the mononuclear complexes (**3**–**5**) to the binuclear complex (**6**). It may well be that correlation (or lack thereof) may be strain-dependent and/or compound-specific. For this reason a larger number of complexes need to be synthesized and tested against a broader range of drug-sensitive and drug-resistant strains of the malaria parasite *P. falciparum*.

A resistance index (RI) value <1 may suggest that cross resistance with chloroquine is unlikely and/or that these complexes will be active against drug resistant strains of the parasite [44]. The RI values of the tested compounds are determined relative to chloroquine, and are calculated by dividing the IC_{50} values for the CQR (Dd2) strain by that of the CQS (NF54) strain. The RI values were calculated for the aryl-derived compounds, and found to be lower than the value for chloroquine diphosphate. All compounds, with the exception of **3**, displayed lower RI values compared to CQ.

3. Conclusions

Imino- and amino-phosphine ligands as well as four new cyclopalladated thiosemicarbazone complexes containing phosphorus ligands have been synthesized and characterized. These complexes were evaluated for their antiplasmodial activity against two *P. falciparum* strains. The mononuclear complexes displayed activity in the low micromolar range, which was significantly more potent than that observed for the binuclear complex. As observed with other cyclopalladated complexes, the biological data for the mononuclear complexes is promising, and thus modifications of these mononuclear complexes may lead to enhanced activity.

4. Experimental

4.1. General remarks

All reagents and solvents were purchased from commercial suppliers and used without further purification. Thiosemicarbazone ligands (**L5**, **L6**) [36], $K_2[PdCl_4]$ [45], the cyclopalladated tetranuclear complexes (**1**,**2**) [19], as well as the iminophosphine ligand (**L1**) [35] were prepared using reported methods. Nuclear magnetic resonance (NMR) spectra were recorded on either a Varian Mercury XR400 MHz (^{1}H: 399.95 MHz) or Bruker Biospin GmbH (^{1}H: 400.22 MHz, ^{13}C: 100.65 MHz, ^{31}P: 162.00 MHz) spectrometer at ambient temperature. ^{1}H and ^{13}C{^{1}H} NMR chemical shifts are referenced to the deuterated solvent. Infrared (IR) spectra were determined using a Perkin–Elmer Spectrum 100 FT-IR spectrometer, and were recorded using KBr pellets. Elemental analyses (C, H, S and N) were recorded on a Thermo Flash 1112 Series CHNS-O Analyser. Electron Impact (EI) mass spectrometry was carried out on a JEOL GCmateII. Electrospray Ionisation (ESI) mass spectrometry was also carried out on a Waters API Quattro Micro triple quadrupole mass spectrometer in the positive mode. Melting points were determined on the Büchi Melting Point apparatus B-540.

4.1.1. Synthesis of N^1,N^4-bis(2-(diphenylphosphino)benzylidene) benzene-1,4-diamine (*L2*)

2-(Diphenylphosphino)benzaldehyde (0.101 g, 0.346 mmol) was added to methanol (15 mL), followed by the addition of benzene-1,4-diamine (0.0186 g, 0.172 mmol). The reaction mixture was refluxed at 68 °C for 6 h, and stirred overnight at ambient temperature to yield a yellow suspension. A light yellow powder was collected by suction filtration, washed with hexane and dried *in vacuo*. Yield: 0.0985 g, 88%. Melting point: 206.4–210.4 °C. ^{1}H NMR (399.95 MHz, $CDCl_3$): δ (ppm) = 9.06 (d, $^4J_{HP}$ = 5.10 Hz, 2H, HC=N); 8.19 (m, 2H, H_d); 7.45 (t, $^3J_{HH}$ = 7.80 Hz, 2H, H_c); 7.33 (m, 22H, PPh_2 & H_b); 6.94 (m, 2H, H_a); 6.88 (s, 4H, H_e). ^{31}P NMR (162.00 MHz, $CDCl_3$): δ (ppm) = −22.2. FT-IR (KBr, cm^{-1}): ν = 3435 (w, N–H); 1610 (m, C=N). MS-EI$^+$: *m*/*z* 653 ([M]$^+$, 40%); 652 ([M − H]$^+$, 94%).

4.1.2. Synthesis of N-(2-(diphenylphosphino)benzyl)propan-1-amine (*L3*)

Compound **L1** (0.0635 g, 0.192 mmol) was dissolved in dry methanol (20 mL), followed by the slow addition of sodium borohydride (0.0127 g, 0.336 mmol). The reaction mixture was stirred at ambient temperature for 3 h. The solvent was removed, the contents of the flask quenched with water (20 mL), and extracted with dichloromethane (3 × 20 mL). The organic layer was collected, washed with water (2 × 15 mL), and dried over anhydrous $MgSO_4$. The solvent was removed to afford a yellow oil which was dried *in vacuo*. Yield: 0.0583 g, 91%. ^{1}H NMR (399.95 MHz, $CDCl_3$): δ (ppm) = 7.58 (m, 1H, H_d); 7.40 (m, 1H, H_c); 7.23 (m, 10H, PPh_2); 7.09 (t, $^3J_{HH}$ = 7.64 Hz, 1H, H_b); 6.83 (dd, J_{HH} = 7.32, 4.39 Hz, 1H, H_a); 3.90 (s, 2H, $-C\underline{H}_2-N$); 2.39 (t, $^3J_{HH}$ = 7.40 Hz, 2H, $N-C\underline{H}_2-$); 1.72 (br s, 1H, NH); 1.26 (m, 2H, $-C\underline{H}_2-$); 0.73 (t, $^3J_{HH}$ = 7.44 Hz, 3H, $-CH_3$). ^{13}C NMR (75.46 MHz, $CDCl_3$): δ (ppm) = 144.6 (d, $^2J_{CP}$ = 24.1 Hz, $\underline{C}_{Ar}-CH_2$); 136.6 (d, $^1J_{CP}$ = 10.1 Hz, PPh_2); 135.6 (d, $^1J_{CP}$ = 13.5 Hz, $\underline{C}_{Ar}-PPh_2$); 133.9 (d, $^2J_{CP}$ = 20.1 Hz, PPh_2); 133.6 (C_d); 129.3 (d, $^2J_{CP}$ = 5.20 Hz, C_a); 128.8 (C_c); 128.7 (PPh_2); 128.5 (d, $^3J_{CP}$ = 6.87 Hz, PPh_2); 127.1 (C_b); 52.7 (d, $^3J_{CP}$ = 20.7 Hz, $-CH_2-N$); 51.4 ($N-CH_2-$); 23.2 ($-CH_2-$); 11.9 ($-CH_3$). ^{31}P NMR (121.47 MHz, $CDCl_3$): δ (ppm) = −16.1. FT-IR (solution, CH_2Cl_2, cm^{-1}): ν = 3405 (w, N–H).

4.1.3. Synthesis of N^1,N^4-bis(2-(diphenylphosphino)benzyl) benzene-1,4-diamine (*L4*)

Compound **L2** (0.0572 g, 0.0876 mmol) was dissolved in dry dichloromethane:methanol (75:25% v/v, 20 mL), followed by the slow addition of sodium borohydride (0.0157 g, 0.415 mmol). The reaction mixture was stirred at ambient temperature for 6 h. The solvent was removed, the contents redissolved in dichloromethane (25 mL), extracted using water (20 mL), and the organic layer was collected. The organic layer was washed with water (4 × 20 mL), and once again collected, and dried over anhydrous $MgSO_4$. The solvent was reduced to precipitate a yellow powder which was collected by suction filtration, washed with hot hexane and dried *in vacuo*. Yield: 0.0543 g, 94%. Melting point: 194.8–198.5 °C. ^{1}H NMR (399.95 MHz, DMSO-d_6): δ (ppm) = 7.60 (m, 4H, H_d); 7.41 (m, 12H, PPh_2); 7.31 (t, $^3J_{HH}$ = 7.80 Hz, 2H, H_c); 7.24 (m, 8H, PPh_2); 7.17 (t, $^3J_{HH}$ = 7.60 Hz, 2H, H_b); 6.76 (dd, J_{HH} = 7.51, 4.76 Hz, 2H, H_a); 6.14 (s, 4H, H_e); 5.30 (br s, 2H, NH); 4.19 (br s, 4H, $-C\underline{H}_2-N$). ^{13}C NMR (100.65 MHz, DMSO-d_6): δ (ppm) = 144.1 (d, $^2J_{CP}$ = 22.0 Hz, $\underline{C}_{Ar}-CH_2$); 139.7 ($\underline{C}_{Ar}-NH$); 135.7 (d, $^1J_{CP}$ = 10.3 Hz, PPh_2); 134.4 (d, $^1J_{CP}$ = 14.7 Hz, $\underline{C}_{Ar}-PPh_2$); 133.5 (d, $^2J_{CP}$ = 19.8 Hz, PPh_2); 132.2 (C_d); 131.3 (d, $^2J_{CP}$ = 9.46 Hz, C_a); 129.0 (C_c); 128.8 (d, $^3J_{CP}$ = 6.60 Hz, PPh_2); 127.0 (d, $^4J_{CP}$ = 4.40 Hz, PPh_2); 126.7 (C_b); 113.5 (C_e); 46.1 (d, $^3J_{CP}$ = 25.7 Hz, $-CH_2-N$). ^{31}P NMR (162.00 MHz, $CDCl_3$): δ (ppm) = −16.9. FT-IR (KBr, cm^{-1}): ν = 3427 (w, N–H); 1517 (s, C=C). MS-EI$^+$: *m*/*z* 656 ([M]$^+$, 40%); 655 ([M − H]$^+$, 100%).

4.1.4. Synthesis of [Pd(3,4-dichloroacetophenone thiosemicarbazone)(PTA)] (*3*)

Compound **1** (0.300 g, 0.205 mmol) was suspended in acetone (15 mL), followed by the addition of 1,3,5-triaza-7-phosphaadamantane (0.123 g, 0.781 mmol) to the reaction flask. The reaction mixture was refluxed at 60 °C for 3 h, and cooled to ambient temperature. The yellow powder was collected by suction filtration, washed with acetone and diethyl ether, and dried *in vacuo*. Yield: 0.383 g, 94%. Melting point: 243.0–248.4 °C. ^{1}H NMR (399.95 MHz, DMSO-d_6): δ (ppm) = 7.27 (s, 1H, H_b); 7.10 (d, $^4J_{HP}$ = 3.42 Hz, 1H, H_a); 7.02 (s, 2H, NH_2); 4.59 (d, J_{HP} = 12.4 Hz, 3H, $NCH_{2(eq)}N$); 4.44 (d, J_{HP} = 13.2 Hz, 3H, $NCH_{2(ax)}N$); 4.27 (s, 6H, PCH_2N); 2.21 (s, 3H, CH_3). ^{13}C NMR (100.65 MHz, DMSO-d_6): δ (ppm) = 177.2 (C–S); 163.7 (C=N); 163.6 (C_{Ar}–Pd); 153.2 ($\underline{C}_{Ar}-CN$); 136.4 (C–Cl); 130.6 (C–Cl); 127.2 (C_a); 127.1 (C_b); 72.4 (d, $^3J_{CP}$ = 7.40 Hz, NCH_2N); 51.5 (d, $^1J_{CP}$ = 15.5 Hz, PCH_2N); 13.6 (CH_3). ^{31}P NMR (162.00 MHz, DMSO-d_6): δ (ppm) = −49.5. FT-IR (KBr, cm^{-1}): ν = 3414 (m, N–H); 1624 (m, C=N); 1574 (w, C=N); 1488 (w, C=C aromatics). Elemental analysis for $C_{15}H_{19}Cl_2N_6PdPS$: Found C 35.0, H 3.46, N 16.4, S 5.91%; Calculated C 34.4, H 3.66, N 16.0, S 6.12%. EI$^+$-MS: *m*/*z* 524 ([M]$^+$, 4%).

4.1.5. Synthesis of [Pd(3,4-dichloropropiophenone thiosemicarbazone)(PTA)] (*4*)

Compound **4** was synthesised following a procedure similar to that described for **3**. Compound **2** (0.0253 g, 0.166 mmol) was reacted with PTA (0.109 g, 693 mmol) to yield a yellow solid. Yield: 0.265 g, 74%. Melting point: 235.9–239.4 °C. ^{1}H NMR (399.95 MHz, DMSO-d_6): δ (ppm) = 7.27 (br s, 1H, H_b); 7.11 (br s, 1H, H_a); 7.05 (s, 2H, NH_2); 4.58 (d, J_{HP} = 12.8 Hz, 3H, $N-CH_{2(eq)}-N$); 4.44 (d, J_{HP} = 12.8 Hz, 3H, $N-CH_{2(ax)}-N$); 4.26 (s, 6H, PCH_2N); 2.70 (q, $^3J_{HH}$ = 7.60 Hz, 2H, CH_2); 1.02 (t, $^3J_{HH}$ = 7.60 Hz, 3H, CH_3). ^{13}C NMR (100.65 MHz, DMSO-d_6): δ (ppm) = 177.4 (C–S); 168.3 (C=N); 164.2 (C_{Ar}–Pd); 151.9 (C_{Ar}–CN); 136.6 (C–Cl); 130.6 (C–Cl); 127.2 (C_a); 127.0 (C_b); 72.4 (d, $^3J_{CP}$ = 7.40 Hz, NCH_2N); 51.5 (d, $^1J_{CP}$ = 15.5 Hz, PCH_2N); 20.0 (CH_2); 11.5 (CH_3). ^{31}P NMR (162.00 MHz, DMSO-d_6): δ (ppm) = −49.6. FT-IR (KBr, cm^{-1}): ν = 3440 (br, N–H); 1641 (w, C=N); 1559 (w, C=N); 1497 (w, C=C aromatics). Elemental analysis for $C_{16}H_{22}Cl_2N_6PdPS$: Found C 35.8, H 4.14, N 16.1, S 5.48%; Calculated C 35.7, H 4.12, N 15.6, S 5.95%. EI$^+$-MS: *m*/*z* 538 ([M]$^+$, 2.4%).

4.1.6. Synthesis of [Pd(3,4-dichloroacetophenone thiosemicarbazone)(N-(2-(diphenylphosphino)benzyl) propan-1-amine)] (**5**)

Compound **L3** (0.131 g, 0.393 mmol) was dissolved in dry acetone (10 mL), followed by the addition of compound **1** (0.143 g, 0.0973 mmol). The reaction mixture was stirred at ambient temperature for 3 h. The volume of the solution was reduced, and the solid precipitated with the addition of hexane. The solid was purified using column chromatography (silica, Ethyl acetate:hexane, 1:1). The yellow powder was collected by suction filtration, and washed with diethyl ether. Yield: 0.108 g, 40%. Melting point: 179.7–184.1 °C. ^{1}H NMR (399.95 MHz, DMSO-d_6): δ (ppm) = 7.74 (m, 1H, H_f); 7.49 (m, 11H, H_c & PPh_2); 7.32 (t, $^3J_{HH}$ = 7.70 Hz, 1H, H_d); 7.23 (s, 1H, H_b); 7.00 (m, 1H, H_e); 6.90 (br s, 2H, NH_2); 6.13 (d, $^4J_{HP}$ = 3.85 Hz, H_a); 4.13 (s, 2H, –$\underline{C}H_2$–NH); 2.28 (m, 2H, NH–$C\underline{H}_2$–CH_2); 2.26 (s, 3H, CH_3); 0.71 (t, $^3J_{HH}$ = 7.28 Hz, 3H, CH_2–$C\underline{H}_3$). ^{13}C NMR (100.65 MHz, DMSO-d_6): δ (ppm) = 177.2 (d, $^3J_{CP}$ = 9.43 Hz, C–S); 172.4 (C=N); 163.7 (C_{Ar}–Pd); 163.6 (d, $^2J_{CP}$ = 4.70 Hz, $\underline{C}_{Ar}$–CH_2); 153.2 ($\underline{C}_{Ar}$–CN); 145.2 (d, $^3J_{CP}$ = 11.4 Hz, C_f); 135.9 (d, $^1J_{CP}$ = 8.10 Hz, $\underline{C}_{Ar}$–PPh_2); 135.0 (d, $^1J_{CP}$ = 12.8 Hz, PPh_2); 132.6 (C_c); 131.7 (C_e); 131.3 (C–Cl); 130.8 (C–Cl); 130.7 (d, $^2J_{CP}$ = 8.10 Hz, PPh_2); 130.1 (d, $^4J_{CP}$ = 3.40 Hz, PPh_2); 129.3 (d, $^2J_{CP}$ = 10.1 Hz, C_a); 127.2 (d, $^3J_{CP}$ = 8.10 Hz, PPh_2); 127.0 (C_d); 126.7 (C_b); 56.2 (NH–$\underline{C}H_2$–CH_2); 52.8 (d, $^3J_{CP}$ = 12.8 Hz, $\underline{C}H_2$–NH); 51.5 (CH_2–$\underline{C}H_2$–CH_3); 13.7 (CH_3); 12.0 (CH_2–$\underline{C}H_3$). ^{31}P NMR (162.00 MHz, DMSO-d_6): δ (ppm) = 29.5. FT-IR (KBr, cm^{-1}): ν = 3435 (w, N–H); 3318 (w, N–H); 1618 (m, C=N); 1582 (w, C=N). Elemental analysis for $C_{31}H_{31}Cl_2N_4PdPS\cdot H_2O\cdot 2C_3H_6O\cdot \frac{1}{2}n\text{-}C_6H_{14}$: Found C 50.8, H 5.17, N 5.92, S 3.59%; Calculated C 50.7, H 4.94, N 6.39, S 3.66%. ESI$^+$-MS: *m/z* 700 ([M]$^+$, 45%); 701 ([M + H]$^+$, 100%).

4.1.7. Synthesis of [Pd_2(3,4-dichloroacetophenone thiosemicarbazone)$_2$(N^1,N^4-bis(2-(diphenylphosphino)benzyl) benzene-1,4-diamine)] (**6**)

Compound **L4** (0.0413 g, 0.0629 mmol) was suspended in an acetone:dichloromethane (80:20% v/v, 10.0 mL) mixture, followed by the addition of compound **1** (0.0459 g, 0.0313 mmol). The reaction mixture was stirred at ambient temperature for 5 h. The yellow powder was collected by suction filtration, washed with hexane and diethyl ether, and dried *in vacuo*. Yield: 0.0507 g, 58%. Melting point: 246.5–249.3 °C. ^{1}H NMR (399.95 MHz, DMSO-d_6): δ (ppm) = 7.50 (m, 24H, H_c & H_f & PPh_2); 7.35 (t, $^3J_{HH}$ = 7.50 Hz, 1H, H_d); 7.21 (s, 1H, H_b); 7.08 (m, 1H, H_e); 6.91 (br s, 2H, NH_2); 6.18 (d, $^4J_{HP}$ = 3.70 Hz, H_a); 5.87 (s, 4H, H_{Ar}); 5.32 (br s, 2H, NH); 4.65 (br s, 2H, –$\underline{C}H_2$–NH); 2.24 (s, 3H, CH_3). ^{13}C NMR (100.65 MHz, DMSO-d_6): δ (ppm) = 177.1 (d, $^3J_{CP}$ = 10.1 Hz, C–S); 164.0 (C=N); 163.5 (d, $^2J_{CP}$ = 4.71 Hz, $\underline{C}_{Ar}$–CH_2); 163.3 (C_{Ar}–Pd); 153.3 ($\underline{C}_{Ar}$–CN); 144.6 (d, $^3J_{CP}$ = 11.4 Hz, C_f); 140.0 (NH–$\underline{C}H_2$–); 135.7 (d, $^1J_{CP}$ = 7.40 Hz, $\underline{C}_{Ar}$–PPh_2); 135.0 (d, $^1J_{CP}$ = 12.1 Hz, PPh_2); 133.0 (d, $^2J_{CP}$ = 3.40 Hz, C_c); 131.8 (C_e); 130.8 (C–Cl); 130.3 (C–Cl); 130.1 (d, $^4J_{CP}$ = 3.89 Hz, PPh_2); 129.3 (d, $^2J_{CP}$ = 10.4 Hz, PPh_2); 128.6 (d, $^3J_{CP}$ = 8.17 Hz, C_a); 127.0 (d, $^3J_{CP}$ = 10.8 Hz, PPh_2); 126.8 (C_d); 126.5 (C_b); 114.0 (–$\underline{C}H_2$–CH_3); 47.9 (d, $^3J_{CP}$ = 14.8 Hz, –$\underline{C}H_2$–NH); 13.8 (CH_3). ^{31}P NMR (162.00 MHz, DMSO-d_6): δ (ppm) = 29.0. FT-IR (KBr, cm^{-1}): ν = 3483 (w, N–H); 3380 (w, N–H); 1597 (m, C=N); 1574 (w, C=N). Elemental analysis for $C_{62}H_{52}Cl_4N_8Pd_2P_2S_2\cdot \frac{1}{2}H_2O$: Found C 53.6, H 4.13, N 7.52, S 3.92%; Calculated C 53.2, H 3.75, N 8.01, S 4.58%. ESI$^+$-MS: *m/z* 1391 ([M + H]$^+$, 12%); 1390 ([M]$^+$, 10%).

4.2. Single-crystal X-ray crystallography

Single-crystal X-ray diffraction data were collected on a Bruker KAPPA APEX II DUO diffractometer using graphite-monochromated Mo-Kα radiation (χ = 0.71073 Å). Data collection was carried out at 173(2) K. Temperature was controlled by an Oxford Cryostream cooling system (Oxford Cryostat). Cell refinement and data reduction were performed using the program SAINT [46]. The data were scaled and absorption correction performed using SADABS [47]. The structure was solved by direct methods using SHELXS-97 [47] and refined by full-matrix least-squares methods based on F2 using SHELXL-97 [47] and using the graphics interface program X-Seed [48,49]. The programs X-Seed and POV-Ray [50] were both used to prepare molecular graphic images. All non-hydrogen atoms were refined anisotropically. All hydrogen atoms were placed at calculated positions with C–H distances ranging from 0.95 Å to 0.99 Å and N–H distance 0.88 Å and refined as riding on their parent atoms with U_{iso} (H) = 1.2 or 1.5 U_{eq} (C or N).

4.3. Antiplasmodial screening

The test samples were tested in triplicate on one occasion against chloroquine sensitive NF54 and chloroquine resistant Dd2 strain of *P. falciparum*. Continuous *in vitro* cultures of asexual erythrocyte stages of *P. falciparum* were maintained using a modified method of Trager et al. [51] Quantitative assessment of antiplasmodial activity *in vitro* was determined via the parasite lactate dehydrogenase assay using a modified method described by Makler et al. [52] The test samples were prepared to a 20 mg/ml stock solution in 100% DMSO and sonicated to enhance solubility. Samples were tested as a suspension if not completely dissolved. Stock solutions were stored at −20 °C. Further dilutions were prepared on the day of the experiment. Chloroquine diphosphate (CQDP) was used as the reference drug in the experiment. A full dose–response was performed for all compounds to determine the concentration inhibiting 50% of parasite growth (IC_{50} value). The samples were tested at a starting concentration of 100,000 ng/ml, which was then serially diluted 2-fold in complete medium to give 10 concentrations; with the lowest concentration being 2 ng/ml. The same dilution technique was used for all samples. The highest concentration of solvent to which the parasites were exposed to had no measurable effect on the parasite viability (data not shown). The IC_{50} values were obtained using a non-linear dose–response curve fitting analysis via Graph Pad Prism v.4.0 software.

Acknowledgements

Financial support from the University of Cape Town and the National Research Foundation (NRF) of South Africa is gratefully acknowledged. We thank the Anglo American Platinum Limited for the kind donation of palladium salts. The South African Research Chairs initiative of the Department of Science and Technology administered through the NRF is gratefully acknowledged for support (K.C.).

Appendix A. Supplementary material

CCDC 923955, 923956 and 923957 contain the supplementary crystallographic data for this paper. These data can be obtained free of charge from The Cambridge Crystallographic Data Centre via www.ccdc.cam.ac.uk/data_request/cif.

References

[1] P. Govender, B. Therrien, G.S. Smith, Eur. J. Inorg. Chem. (2012) 2853–2862.
[2] C.G. Hartinger, A.D. Phillips, A.A. Nazarov, Curr. Top. Med. Chem. 11 (2011) 2688–2702.
[3] F.K. Keter, J. Darkwa, Biometals 25 (2012) 9–21.
[4] C.S. Allardyce, P.J. Dyson, Top. Organomet. Chem. 17 (2006) 177–210.
[5] World Health Organisation http://www.who.int/malaria/world_malaria_report_2011/WMR2011 (accessed January 2013).
[6] J.N. Burrows, K. Chibale, T.N.C. Wells, Curr. Top. Med. Chem. 11 (2011) 1226–1254.

[7] G. Gasser, N. Metzler-Nolte, Curr. Opin. Chem. Biol. 16 (2012) 84–91.
[8] C. Biot, W. Castro, C.Y. Botte, M. Navarro, Dalton Trans. 41 (2012) 6335–6349.
[9] M. Navarro, W. Castro, C. Biot, Organometallics 31 (2012) 5715–5727.
[10] P. Chellan, K.M. Land, A. Shokar, A. Au, S.H. An, C.M. Clavel, P.J. Dyson, C. de Kock, P.J. Smith, K. Chibale, G.S. Smith, Organometallics 31 (2012) 5791–5799.
[11] P. Chellan, N. Shunmoogam-Gounden, D.T. Hendricks, J. Gut, P.J. Rosenthal, C. Lategan, P.J. Smith, K. Chibale, G.S. Smith, Eur. J. Inorg. Chem. (2010) 3520–3528.
[12] T. Stringer, P. Chellan, B. Therrien, N. Shunmoogam-Gounden, D.T. Hendricks, G.S. Smith, Polyhedron 28 (2009) 2839–2846.
[13] R.W. Brockman, J.R. Thomson, M.J. Bell, H.E. Skipper, Cancer Res. 16 (1956) 167–170.
[14] A.I. Matesanz, P. Souza, Mini-Rev. Med. Chem. 9 (2009) 1389–1396.
[15] T. Stringer, B. Therrien, D.T. Hendricks, H. Guzgay, G.S. Smith, Inorg. Chem. Commun. 14 (2011) 956–960.
[16] P. Genova, T. Varadinova, A.I. Matesanz, D. Marinova, P. Souza, Toxicol. Appl. Pharmacol. 197 (2004) 107–112.
[17] C. Shipman Jr., S.H. Smith, J.C. Drach, D.L. Klayman, Antimicrob. Agents Chemother. 19 (1981) 682–685.
[18] S.A. Khan, M. Yusuf, Eur. J. Med. Chem. 44 (2009) 2270–2274.
[19] P. Chellan, S. Nasser, L. Vivas, K. Chibale, G.S. Smith, J. Organomet. Chem. 695 (2010) 2225–2232.
[20] D.C. Greenbaum, Z. Mackey, E. Hansell, P. Doyle, J. Gut, C.R. Caffrey, J. Lehrman, P.J. Rosenthal, J.H. McKerrow, K. Chibale, J. Med. Chem. 47 (2004) 3212–3219.
[21] R.B. de Oliveira, E.M. de Souza-Fagundes, R.P.P. Soares, A.A. Andrade, A.U. Krettli, C.L. Zani, Eur. J. Med. Chem. 43 (2008) 1983–1988.
[22] A. Chipeleme, J. Gut, P.J. Rosenthal, K. Chibale, Bioorg. Med. Chem. 15 (2007) 273–282.
[23] I. Chiyanzu, E. Hansell, J. Gut, P.J. Rosenthal, J.H. McKerrow, K. Chibale, Bioorg. Med. Chem. Lett. 13 (2003) 3527–3530.
[24] D.L. Klayman, J.F. Bartosevich, T.S. Griffin, C.J. Mason, J.P. Scovill, J. Med. Chem. 22 (1979) 855–862.
[25] Z. Kovacevic, D.S. Kalinowski, D.B. Lovejoy, P. Quach, J. Wong, D.R. Richardson, Curr. Drug Deliv. 7 (2010) 194–207.
[26] Y. Yu, D.S. Kalinowski, Z. Kovacevic, A.R. Siafakas, P.J. Jansson, C. Stefani, D.B. Lovejoy, P.C. Sharpe, P.V. Bernhardt, D.R. Richardson, J. Med. Chem. 52 (2009) 5271–5294.
[27] J. Dupont, C.S. Consorti, J. Spencer, Chem. Rev. 105 (2005) 2527–2571.
[28] T.S. Lobana, G. Bawa, G. Hundal, R.J. Butcher, A. Castineiras, Z. Anorg. Allg. Chem. 635 (2009) 1447–1453.
[29] T.S. Lobana, G. Bawa, G. Hundal, M. Zeller, Z. Anorg. Allg. Chem. 634 (2008) 931–937.
[30] T.S. Lobana, G. Bawa, G. Hundal, M. Zeller, Organometallics 27 (2008) 175–180.
[31] T.S. Lobana, P. Kumari, R.J. Butcher, T. Akitsu, Y. Aritake, J. Perles, F.J. Fernández, M.C. Vega, J. Organomet. Chem. 701 (2012) 17–26.
[32] F. Mohr, S.H. Priver, S.K. Bhargava, M.A. Bennett, Coord. Chem. Rev. 250 (2006) 1851–1888.
[33] C. Navarro-Ranninger, I. López-Solera, V.M. González, J.M. Pérez, A. Alvarez-Valdés, A. Martín, P.R. Raithby, J.R. Masaguer, C. Alonso, Inorg. Chem. 35 (1996) 5181–5187.
[34] A.G. Quiroga, J.M. Pérez, I. López-Solera, J.R. Masaguer, A. Luque, P. Román, A. Edwards, C. Alonso, C. Navarro-Ranninger, J. Med. Chem. 41 (1998) 1399–1408.
[35] C.A. Ghilardi, S. Midollini, S. Moneti, A. Orlandini, G. Scapacci, J. Chem. Soc. Dalton Trans. 1 (2001) 3371–3378.
[36] X. Du, C. Guo, E. Hansell, P.S. Doyle, C.R. Caffrey, T.P. Holler, J.H. McKerrow, F.E. Cohen, J. Med. Chem. 45 (2002) 2695–2707.
[37] T. Stringer, D.T. Hendricks, H. Guzgay, G.S. Smith, Polyhedron 31 (2012) 486–493.
[38] R. Schibli, K.V. Katti, W.A. Volkert, C.L. Barnes, Inorg. Chem. 37 (1998) 5306–5312.
[39] P. Smolenski, A.J.L. Pombeiro, Dalton Trans. 1 (2008) 87–91.
[40] L.A. Adrio, A. Amoedo, J.M. Antelo, J.J. Fernández, J. Martínez, J.M. Ortigueira, M.T. Pereira, J.M. Vila, Z. Anorg. Allg. Chem. 631 (2005) 2204–2209.
[41] J. Martínez, L.A. Adrio, J.M. Antelo, J.M. Ortigueira, M.T. Pereira, J.J. Fernández, A. Fernández, J.M. Vila, J. Organomet. Chem. 691 (2006) 2721–2733.
[42] H. Weiss, F. Mohr, J. Organomet. Chem. 696 (2011) 3150–3154.
[43] L. Adrio, G. Alberdi, A. Amoedo, D. Lata, A. Fernández, J. Martínez, M.T. Pereira, J.M. Vila, Z. Anorg. Allg. Chem. 631 (2005) 2197–2203.
[44] C. Herrmann, P.F. Salas, J.F. Cawthray, C. de Kock, B.O. Patrick, P.J. Smith, M.J. Adam, C. Orvig, Organometallics 31 (2012) 5748–5759.
[45] M.G. Abdullaev, Pharm. Chem. J. 35 (2001) 45–48.
[46] SAINT Version 7.60a, Bruker AXS Inc., Madison, WI, USA, 2006.
[47] G.M. Sheldrick, SHELXL-97 and SHELXS-97, Program for Crystal Structure Refinement, University of Göttingen, Germany, 1997.
[48] L.J. Barbour, J. Supramol. Chem. 1 (2001) 189–191.
[49] J.L. Atwood, L.J. Barbour, Cryst. Growth Des. 3 (2003) 3–8.
[50] http://www.povray.org.
[51] W. Trager, J.B. Jensen, Science 193 (1976) 673–675.
[52] M.T. Makler, J.M. Ries, J.A. Williams, J.E. Bancroft, R.C. Piper, B.L. Gibbins, D.J. Hinrichs, Am. Soc. Trop. Med. Hyg. 48 (1993) 739–741.